Acta Biomaterialia xxx (xxxx) xxx

Contents lists available at ScienceDirect

Acta Biomaterialia

journal homepage: www.elsevier.com/locate/actabiomat

Full length article

Micro-injection molded, poly(vinyl alcohol)-calcium salt templates for precise customization of 3D hydrogel internal architecture ☆

Jason D. McNulty [a,b,1], Carlos Marti-Figueroa [a,c,1], Frank Seipel [a,c], Joshua Z. Plantz [a,c], Thomas Ellingham [a,b], Lukas J.L. Duddleston [b], Sebastian Goris [b], Benjamin L. Cox [d,e], Tim A. Osswald [b], Lih-Sheng Turng [a,b], Randolph S. Ashton [a,c,*]

[a] Wisconsin Institute for Discovery, University of Wisconsin-Madison, Madison, WI 53706, USA
[b] Department of Mechanical Engineering, University of Wisconsin-Madison, Madison, WI 53706, USA
[c] Department of Biomedical Engineering, University of Wisconsin-Madison, Madison, WI 53706, USA
[d] Department of Medical Physics, University of Wisconsin-Madison, Madison, WI 53706, USA
[e] Morgridge Institute for Research, University of Wisconsin-Madison, Madison, WI 53706, USA

ARTICLE INFO

Article history:
Received 31 October 2018
Received in revised form 16 April 2019
Accepted 23 April 2019
Available online xxxx

Keywords:
Alginate
Sacrificial molding
Tissue engineering
Neural organoids

ABSTRACT

In tissue engineering applications, sacrificial molding of hydrogel monoliths is a versatile technique for creating 3D molds to control tissue morphology. Previous sacrificial templates fabricated by serial processes such as solvent casting and thermal extrusion/fiber drawing can be used to effectively mold internal geometries within rapidly polymerizing, bulk curing hydrogels. However, they display poorer performance in controlling the geometry of diffusion limited, ionically cross-linked hydrogels, such as alginate. Here, we describe the use of poly(vinyl alcohol)-calcium salt templates (PVOH-Ca) fabricated by micro-injection molding, a parallel mass-production process, to conveniently cast internal geometries within both bulk curing hydrogels and ionically cross-linked alginate hydrogels. Calcium salt solubility was discovered to be a critical factor in optimizing the polymer composite's manufacturability, mechanical properties, and the quantity of calcium released upon template dissolution. Metrological and computed tomography (CT) analysis showed that the template's calcium release enables precise casting of microscale channel geometries within alginate hydrogels (6.4 ± 7.2% average error). Assembly of modular PVOH-Ca templates to mold 3D channel networks within alginate hydrogels is presented to demonstrate engineering scalability. Moreover, the platform is used to create hydrogel molds for engineering human embryonic stem cell (hESC)-derived neuroepithelial organoids of a microscale, biomimetic cylindrical morphology. Thus, injection molded PVOH-Ca templates facilitate customization of hydrogel sacrificial molding, which can be used to generate 3D hydrogels with complex internal microscale architecture for diverse tissue engineering applications.

Statement of Significance

Sacrificial molding of hydrogel monoliths is a versatile technique for creating 3D molds for tissue engineering applications. Previous sacrificial materials fabricated by serial processes have been used to effectively mold internal geometries within rapidly polymerizing, bulk curing hydrogels. However, they display poor performance in molding geometry within diffusion limited, ionically cross-linked hydrogels, e.g. alginate. We describe the use of poly(vinyl alcohol)-calcium salt templates (PVOH-Ca) fabricated by micro-injection molding, an unparalleled mass-production process, to conveniently cast internal geometries within both bulk curing hydrogels and ionically cross-linked alginate hydrogels. Calcium release from the PVOH-Ca templates enables precise sacrificial molding of alginate hydrogels and the process is biocompatible. Moreover, we demonstrate its use to engineer the morphology of hPSC-derived neuroepithelial organoids, and modular PVOH-Ca template designs can be assembled to enable scalable 3D customization of hydrogel internal architecture.

☆ Part of the Cell and Tissue Biofabrication Special Issue, edited by Professors Guohao Dai and Kaiming Ye.

* Corresponding author at: Department of Biomedical Engineering, University of Wisconsin-Madison, Madison, WI 53706, USA.
E-mail address: rashton2@wisc.edu (R.S. Ashton).

[1] Equal contribution.

https://doi.org/10.1016/j.actbio.2019.04.050
1742-7061/

1. Introduction

Hydrogel biomaterials are used throughout the tissue engineering field as versatile scaffolds to support three-dimensional (3D) cell growth and shape the morphology of tissue constructs [1–6]. *In vivo*, normal tissue development and physiology relies upon proper cytoarchitectural organization at multiple length scales [7]. Hence, several methods have been developed for engineering the macro-to-microscale architecture of hydrogel scaffolds, including layer-by-layer 3D printing technologies, such as fused deposition modeling (FDM) and stereolithography (SLA) [1,3,8,9]. Recently, these methods have been used to fabricate sacrificial templates that enable unprecedented, rapid casting of intricate architectures within hydrogel monoliths [3,10,11]. For example, Miller et al. used a FDM printer to create interconnected 3D lattices composed of water-soluble carbohydrate glass filaments [3]. Subsequently, the lattices could be encapsulated within hydrogels, and upon dissolution, leave behind channel networks suitable for generating microvasculature within prospective 3D tissues. Alternatively, sacrificial poly(vinyl alcohol) (PVOH), alginate, gelatin, and polyethylene glycol (PEG) templates casted within SLA fabricated molds have also been developed to engineer microscale hydrogel architecture [12–15].

While these approaches enable casting of complex hydrogel architectures, the fabrication techniques and sacrificial template materials impose several limitations. First, FDM and SLA/solvent casting fabrication techniques are not easily scaled for mass production due to extended manufacturing cycle times per sacrificial template. Second, carbohydrate glass templates are brittle and inelastic nature, suggesting limited durability during normal handling, whereas those of PVOH and alginate templates were not directly determined [3,12,13]. Third, current sacrificial template materials have only been proven to effectively cast complex geometries within bulk curing hydrogels such as PEG, fibrin, and methacrylated gelatin [3,14]. Poorer dimensional fidelity was observed when Miller et al. used carbohydrate glass lattices to cast channels within diffusion limited, ionically crosslinked alginate hydrogels, a widely used tissue engineering scaffold and clinically approved biomaterial [3,5,12,16,17]. Alginate in particular has several advantageous biomaterial properties for tissue engineering applications: facile and gentle cell encapsulation, ease of chemical modification via densely presented carboxylic acid groups, and enzymatic degradation mechanisms that are orthogonal to the mammalian genome [5,17]. Thus, there remains a need to develop a scalable mass production process for generating durable sacrificial templates capable of accurately casting internal architectural features within both bulk curing and diffusion limited, ionically crosslinked hydrogels.

To address these limitations, we have developed micro-injection molded PVOH-calcium salt composites (PVOH-Ca) as enhanced sacrificial templates for engineering 3D hydrogel molds with complex internal architecture (Schematic 1). Injection molding processes are unmatched in manufacturing scalability due to their automated, parallel production of finished polymer components within seconds [18–20]. Interestingly, calcium salt solubility was discovered to be a critical parameter in optimizing the PVOH-Ca composite's micro-injection molding processability and the resulting templates' durability and casting efficacy. PVOH composited with calcium acetate ($Ca(C_2H_3O_2)_2$) salts produced templates with enhanced mechanical properties and calcium release upon aqueous dissolution, which accelerated the curing rate of alginate hydrogels at the template/hydrogel interface. PVOH-$Ca(C_2H_3O_2)_2$ templates were observed to cast 500 μm diameter channels within alginate hydrogel monoliths with an average dimensionality error of only 6.4 ± 7.2%, and equivalent performance was observed within bulk curing polyacrylamide hydrogels. To demonstrate process scalability and versatility, modular PVOH-$Ca(C_2H_3O_2)_2$ templates were injection molded, assembled into multicomponent Lego®-like structures, and used to generate 3D channel networks within alginate and polyacrylamide hydrogels. The biocompatibility of the PVOH-$Ca(C_2H_3O_2)_2$ template-mediated hydrogel molding process was demonstrated in the presence of hESC-derived neurospheres. Additionally, the templates were used to engineer hESC-derived neuroepithelial organoids with a biomimetic, microscale cylindrical morphology. These results demonstrate the utility, biocompatibility, and versatility of PVOH-calcium acetate templates for sacrificially molding hydrogels with custom internal architectures for tissue engineering applications.

2. Materials and methods

2.1. Materials

Sterile Pronova SLG1000 sodium alginate was purchased from Pronova Biopolymer. Calcium salts ($CaCO_3$, $Ca(C_2H_3O_2)_2$, CaI_2 and $CaCl_2$), Eriochrome Black T, Ammonium Chloride, and Magnesium Chloride were purchased from Sigma Aldrich. Calcium sulfate and ammonia were purchased from Acros Organics. Polyacrylamide, tetramethylethylenediamine (TEMED), and ammonium persulfate were purchased from Biorad. Functionalized PEG-norbornene hydrogel materials were kindly provided by Prof. William Murphy (UW–Madison). Polypropylene 6061 aluminum and 316 stainless steel raw materials were purchased from McMaster-Carr Supply Company. Dexron-VI automatic transmission fluid (ATF) was purchased from Autozone and used as the imaging contrast dye for alginate perfusion.

2.2. Extrusion compounding

Calcium salts were ground via mortar and pestle and sieved until less than 300 μm in dimension. The salts were hand mixed with PVOH (Monopol C100, Monosol Inc.) and conditioned under vacuum at 70 °C for 4 h. The mixture was fed through a volumetric feeder (Tuf-Flex 100, Schenck Accurate) into a co-rotating twin screw compounding extruder (18 mm Leistritz AG) equipped with a screw designed with only feedforward elements and a 6 mm strand die (Schematic 1). Post compounding, the extrudate was run through a pelletizer to prepare the composite for injection molding. Compounding parameters are listed in Supplemental Table S1.

2.3. Mechanical and thermal analysis

Tensile properties were measured using an Instron 5967 Universal Tensile Testing Machine (30 kN) with injection molded ASTM D638 Type V tensile bars elongated at 50 mm/min [21]. Thermogravimetric analysis (TGA) was performed on PVOH-Ca composite samples ranging from 20 to 60 mg within platinum pans (DSC Consumables Inc.) ramped to 600 °C at 10 °C/min (Q50 TGA, TA Instruments). Differential scanning calorimetry (DSC) was performed using hermetic aluminum pans (DSC Consumables Inc.) between 0 and 210 °C at a ramp rate of 10 °C/min (Auto Q20, TA Instruments). Viscosity characterization was performed with a parallel plate rheometer (AR2000, TA Instruments) using injection molded discs with a 24.5 mm diameter and 2 mm thickness.

2.4. Micro-injection molding

Custom injection molds were designed with 3D modeling software (Solidworks 2014, Dassault Systems) and fabricated from

Please cite this article as: J. D. McNulty, C. Marti-Figueroa, F. Seipel et al., Micro-injection molded, poly(vinyl alcohol)-calcium salt templates for precise customization of 3D hydrogel internal architecture, Acta Biomaterialia, https://doi.org/10.1016/j.actbio.2019.04.050

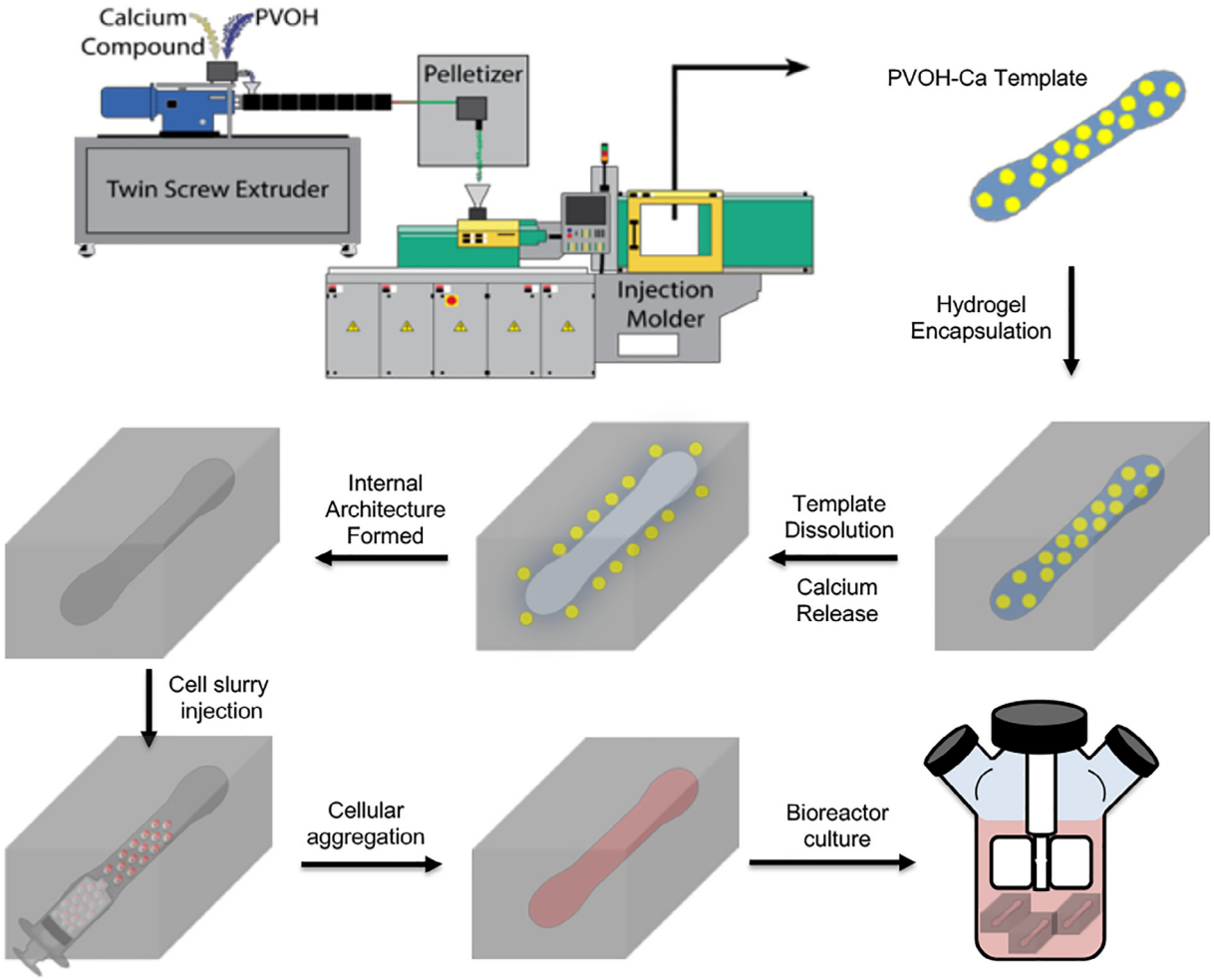

Schematic 1. Illustration of PVOH and calcium salt compounding followed by injection molding of a sacrificial PVOH-Ca template, which is subsequently encapsulated and dissolved within an alginate hydrogel monolith. Release of calcium ions at the hydrogel-template interface enhances interior lumen molding fidelity. The resulting engineered hydrogel can then be used to mold the microscale morphology of hPSC-derived cell aggregates/organoids.

6061 aluminum blocks with a computer numerical control (CNC) vertical machining center (MiniMill 2, Haas) programmed using computer aided design/manufacturing (CAD/CAM) software (Master CAM X7, CNC Software, Inc.). All micro-injection molding was performed on a 38 ton Arburg Allrounder 270A machine with an 18 mm injection unit using processing parameters found in Supplemental Table S1.

2.5. Complexometric calcium titration

A complexometric titration was performed to quantify the amount of Ca ions released from PVOH-Ca templates upon dissolution. 1.4 g of each composite was completely dissolved in 50 mL of deionized water. Then, 100 mL of 50 mM ethylenediaminetetraacetic acid (EDTA) was added to the solution to chelate all free Ca atoms. Eriochrome black T (EBT), a weaker chelating agent used as an indicator, was subsequently added to the solution causing a blue color that changes to pink upon its complexing with cations. Then, $MgCl_2$ was titrated into the solution to react with the excess EDTA to completion, which was indicated by the solution's color change due to Mg's reaction with EBT. Once the solution turned pink, we could estimate the amount of Ca released upon PVOH-Ca template dissolution from the amount of titrated $MgCl_2$. For each template composition, the titration results were compared with the total Ca salt content detected by thermogravimetric analysis (TGA).

2.6. Hydrogel fabrication

2.6.1. Polyacrylamide

Polyacrylamide hydrogels were fabricated within custom polypropylene devices that suspended PVOH templates between inlet and outlet needles (Fig. 1A). Five milliliters of 12% acrylamide/bisacrylamide was prepared, and 100 μL of ammonium persulfate and 4 μL of TEMED were added to initiate the bulk polymerization reaction. After 5 min, the polyacrylamide solution was added to the device to completely encapsulate the suspended PVOH template. The solution was allowed to polymerize for one hour. Then, the device was transferred to a 45 °C water bath and incubated overnight for PVOH dissolution.

2.6.2. Polyethylene glycol (PEG)

PEG-norbornene (PEG-NB) hydrogels were fabricated within custom stainless steel devices that suspended PVOH templates between inlet and outlet needles (Fig. 1B). 4.5 mL of 4% (w/v) PEG-NB was prepared to achieve 60% crosslinking [22]. The solution was added to the device to completely encapsulate the suspended PVOH template. The device was placed under a UV lamp and exposed to UV light at 365 nm wavelength for 20 s to induce polymerization. Then, the device was transferred to a 45 °C water bath and incubated overnight for PVOH dissolution. Post dissolution, the internal channel network was perfused with a mixture of green food colorant and water to enhance imaging contrast.

Please cite this article as: J. D. McNulty, C. Marti-Figueroa, F. Seipel et al., Micro-injection molded, poly(vinyl alcohol)-calcium salt templates for precise customization of 3D hydrogel internal architecture, Acta Biomaterialia, https://doi.org/10.1016/j.actbio.2019.04.050

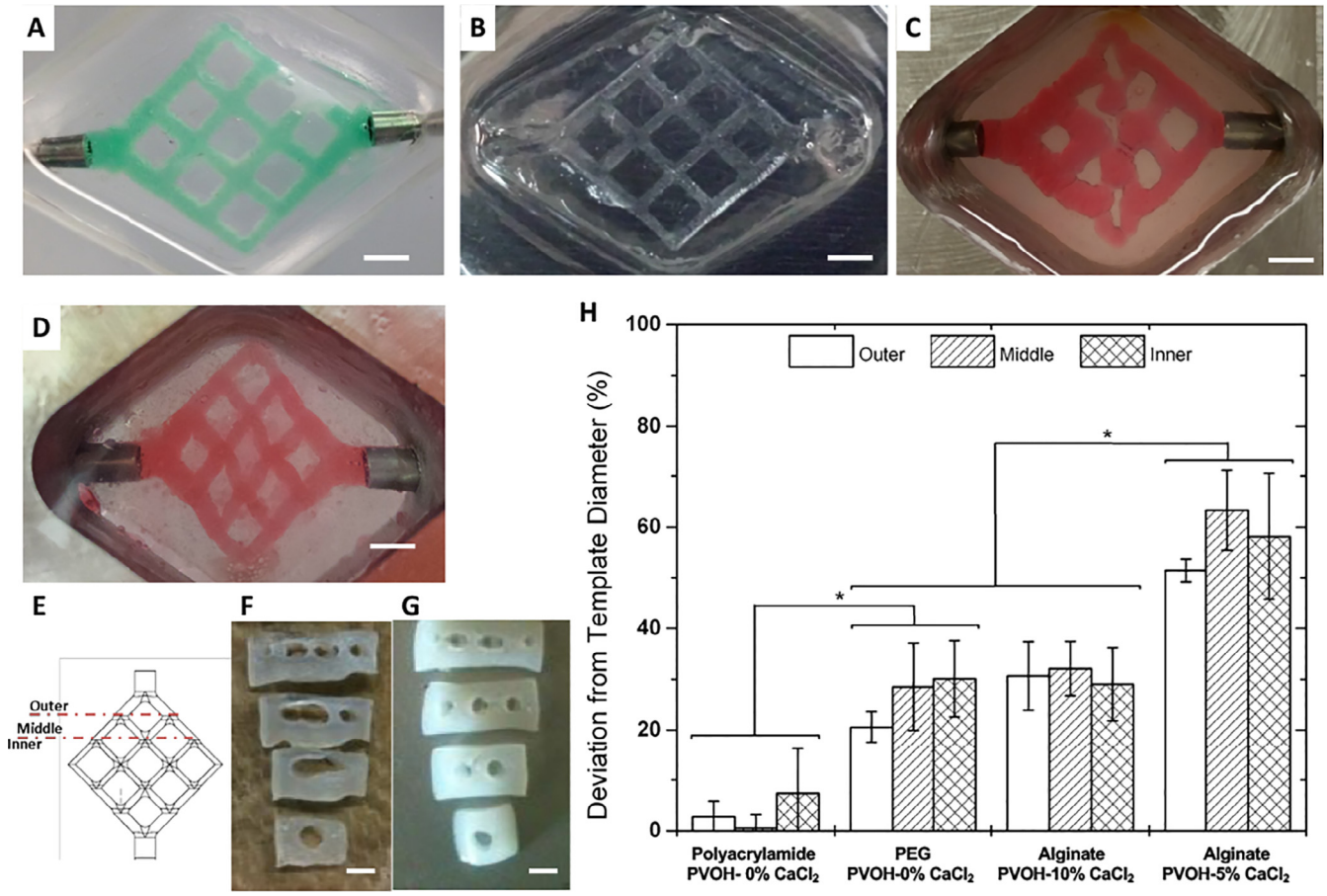

Fig. 1. Channel laden hydrogels molded using PVOH and PVOH-$CaCl_2$ sacrificial templates. (A) polyacrylamide, (B) PEG, and (C) alginate hydrogels cast using PVOH lattices. (D) Alginate hydrogel cast using a 10% (w/w) loaded PVOH-$CaCl_2$ template. (E) Schematic of cross-sectional hydrogel slices made to measure outer, middle, and interior channel diameters. Representative cross-sectional images of alginate hydrogels cast using (F) PVOH and (G) 10% PVOH-$CaCl_2$ templates. (H) Percent deviation of hydrogel channels' diameter from the sacrificial template's dimensions. Data combined from duplicate experiments to yield n = 8, 16 and 24 for outer, middle and inner channels, respectively. Error bars represent standard deviation; $^{*}P < 0.05$, One-way ANOVA with post-hoc Tukey-Kramer test; Scale bars are 3 mm.

2.6.3. Alginate

Alginate hydrogels were fabricated within custom polypropylene and stainless steel devices that suspended PVOH templates between inlet and outlet ports. To form alginate hydrogels, a 5 mL solution of 2% sodium alginate in sterile, deionized water was prepared by overnight mixing at 4 °C. A $CaSO_4$-alginate slurry was prepared by adding 300 μL of 7.5% $CaSO_4$ in deionized water to the 5 mL of 2% sodium alginate solution. The slurry was pipetted into the device to encapsulate the suspended PVOH template, and allowed to pre-gel for 10 min. Then the device was submerged in a room-temperature bath of 2% (w/v) $CaCl_2$ in deionized water overnight to induce bulk hydrogel gelation and completely dissolve the PVOH template. Post dissolution, the internal channel network was perfused with Dexron-VI automatic transmission fluid to enhance imaging contrast. For cell culture studies, stainless steel devices and components are autoclaved, and the devices are assembled and injected with Sodium Alginate and Calcium Chloride solutions in a sterile cell culture hood. The PVOH templates are sterilized in a cell cultured hood with UV for 1hr prior to assembly into stainless steel device.

2.6.4. Hydrogel imaging and reconstruction

Hydrogels were imaged using standard photography or a Micro-CATII (Siemens AG.) at the University of Wisconsin Carbone Cancer Center's small animal imaging facility. The Digital Imaging and Communications in Medicine (DICOM) image stacks were then reconstructed and converted into STL graphic bodies using Mimics software (Materialize NV.). Image analysis was performed using a combination of Magics (Materialize NV.), MeshLabs, and Solidworks (Dassault Systemes).

2.7. Neuroepithelial cell derivation

WA09 (H9, WiCell) human embryonic stem cells (Passage 28–40) were maintained in the pluripotent state in E8 medium (Thermofisher) on Matrigel™ (WiCell) coated plates. The H9 line was authenticated as karyotypically normal by the provider and within 6 months of these experiments and tested for mycoplasma with negative results (WiCell). After banking, the cells were used for no more than 15 passages during experimentation. Neural induction was executed as previously described [23]. Briefly, hESCs were passaged with Accutase (Life Technologies) onto matrigel-coated plates at a density of $1x10^5$ cells/cm^2 with 10 mM ROCK inhibitor (Y27632; R&D Systems). The following day, cells were changed to E6 medium (ThermoFisher) for 4 days with daily, complete media changes.

2.8. Formation of organoids in alginate hydrogel channels

Neuroepithelial cells (NECs) were washed with 2 mL PBS, accutased for 5 min, and removed from the surface by gentle pipetting. After collection by centrifugation, cells were gently resuspended at

Please cite this article as: J. D. McNulty, C. Marti-Figueroa, F. Seipel et al., Micro-injection molded, poly(vinyl alcohol)-calcium salt templates for precise customization of 3D hydrogel internal architecture, Acta Biomaterialia, https://doi.org/10.1016/j.actbio.2019.04.050

a concentration of 250,000 cells/μL in E8 medium containing 10 μM Y27632 and 1:200 Penicllin-Streptomycin (Penstrep, 10,000U/mL) (Invitrogen). Using a PHD Ultra™ syringe pump (Harvard Apparatus) loaded with a 3 cc syringe connected via tubing to a 1–200 μL gel-loading pipette tip (VWR, Cat. No. 37001-150), the cells were collected and injected into the alginate hydrogel's molded channel at a rate of 5–50 nL/s in a sterile environment. The injection process was visualized using an EVOS™ XL Core Imaging System (ThermoFisher). After injection, the hydrogels were removed from their stainless steel devices and cultured in E8 media in 6-well plates for the first 24 hrs. Then, they were transferred to a sterile 125 mL Pyrex Spinner flask (ThermoFisher) agitated on an orbital shaker (Scilogex, Cat. No. SK-0330-Pro) for an additional 4, 8, or 16 days in E6 medium containing 1:200 Penstrep. Complete media changes were conducted every third day.

2.9. Organoid fixation and immunochemistry

After culture, hydrogels containing organoids were washed with PBS 3 times for 10 min, and subsequently fixed with paraformaldehyde (PFA) for 15 min. After fixation, hydrogels were transferred to a 30% sucrose-PBS solution for 1–3 days. Next, the organoids were removed from the hydrogels by incubation in a 100 mM EDTA solution for 1hr, collected by gentle pipetting using a cut 1000 μL pipette tip, and embedded in OCT compound (Sigma-Aldrich) until sectioning. Organoids were sectioned as 30 μm thick slices onto Superfrost Plus microscope slides (ThermoFisher). The slides were washes 3 times with PBS to remove OCT, blocked with TBSDT (Tris Buffered Saline + 5% Donkey Serum + 0.3% Triton X), and incubated in primary antibodies against mouse-anti-N-Cadherin (BD Biosciences, Cat. No. 610920) and rabbit-anti-Pax6 (Biolegend, Cat. No. 901301), or mouse-anti-N-Cadherin and rabbit-anti-Laminin (Abcam, Cat. No. ab30320) for 3 days. All primary antibodies were used at a 1:200 dilution. After incubation, the slides were washed 5 times with TBST (TBS + 0.3% Triton X) and incubated for 1 day in secondary antibodies Alexa 488® donkey-anti-mouse and Alexa 555® donkey-anti-rabbit (1:250, ThermoFisher) and stained with DAPI (Invitrogen, Cat. No. D1306) for 20 min prior to washing with TBS 5 times. Slides were mounted using Prolong Gold anti-fade (ThermoFisher) under No. 1 coverslips (ThermoFisher) and imaged using a Nikon AR1 confocal microscope.

2.10. Statistical analysis

RStudio® was used to conduct all statistical analysis. Experimental replicates or number of groups are detailed in figure legends, and error bars show standard deviations. One-way ANOVAs with post-hoc Tukey-Kramer tests were conducted to determine statistical significance. $P < 0.05$ was considered statistically significant.

3. Results

3.1. Injection molded, sacrificial PVOH and PVOH-$CaCl_2$ templates

In contrast to brittle carbohydrate glass sacrificial templates [3], we opted to produce sacrificial templates using durable, water-soluble, and biocompatible PVOH similar to Tocchio et al. [12]. Micro-injection molding was chosen as the fabrication technique to mitigate manufacturing scalability concerns. Aluminum molds were CNC-milled to produce sacrificial PVOH templates with a lattice geometry consisting of cylinders that transitioned from 3 to 1 mm in diameter (Fig. 1E, and Supplemental Fig. S1). To evaluate their hydrogel molding utility, the templates were encapsulated within polyacrylamide, PEG, and alginate monoliths, and dissolved overnight in a water bath to generate hydrogels with replicate internal architecture. Post template dissolution, bulk curing polyacrylamide and PEG hydrogels displayed discernable internal channel lattice networks (Fig. 1A-B). The PEG hydrogel's channels displayed a higher deviation from the PVOH template's dimensions presumably due to the hydrogel's characteristic swelling [22,24] (Fig. 1H). However, a series of disconnected and non-uniform voids were generated in alginate hydrogels, suggesting that the PVOH template dissolved prior to the inward diffusion of crosslinking Ca^{2+} ions (Fig. 1C and E–F).

To enable effective sacrificial molding of alginate hydrogels, we hypothesized that compounding calcium salts into the PVOH template material would accelerate the crosslinking rate at the template/hydrogel interface and enable more precise sacrificial molding. PVOH was compounded with 5% and 10% (w/w) $CaCl_2$ using twin screw extrusion, and the PVOH-$CaCl_2$ composite was injection molded into a lattice geometry (Fig. 1E). Sacrificial molding with PVOH-$CaCl_2$ templates yielded continuous channel networks within alginate hydrogels indicating that release of the compounded calcium ameliorated casting efficacy (Fig. 1D–G). Metrological analysis of cross-sectioned hydrogels (Fig. 1E–G) revealed that compounding 10% vs. 5% (w/w) $CaCl_2$ into the PVOH lattice template significantly improved molding of the channel network geometry (Fig. 1H). However, the casted architecture's dimensions still deviated from those of the PVOH-$CaCl_2$ template by ~30%. Thus, the addition of $CaCl_2$ to PVOH template material significantly improved molding of internal architecture within ionically crosslinked alginate hydrogels, but the molding fidelity could be further improved.

3.2. Optimizing mechanical properties of PVOH-Ca templates

Although the PVOH-$CaCl_2$ sacrificial molding results were promising, the addition of $CaCl_2$ into the PVOH substrate also yielded undesirable fabrication side effects. Notably, the composite was much more difficult to process via extrusion and injection molding than neat PVOH material. For example, thermal degradation of the 10% PVOH-$CaCl_2$ composite was apparent both visually and aromatically. According to a prior cement study, dissolved Ca^{2+} ions can produce crosslinking-like interactions between hydroxyl groups within the PVOH polymer backbone [25]. Since $CaCl_2$ solubility in water is high and increases with temperature (Supplemental Table S2), it was hypothesized that the thermal processing of extrusion and injection molding amplified Ca^{2+} crosslinking within the polymer composite. Increased polymer chain cross-linking would make PVOH-$CaCl_2$ templates more difficult to injection mold, and it could decrease the release of Ca^{2+} ions upon the templates' aqueous dissolution. Therefore, we investigated whether compounding PVOH with calcium salts of lower solubility would minimize crosslinking interactions during material processing. PVOH was compounded with 10% (w/w) calcium iodide (CaI_2), calcium acetate ($Ca(C_2H_3O_2)_2$), or calcium carbonate ($CaCO_3$) salts, which are listed in order of decreasing solubility (Supplemental Table S2), and each composites' mechanical and calcium release properties were analyzed in detail (Figs. 2 and 3).

Tensile strength tests on injection molded PVOH-Ca ASTM D638 Type V specimens showed that the compounded calcium salts decrease the material's ductility, i.e. strain at break, and increase its modulus and ultimate axial tensile strength (UTS) compared to neat PVOH (Fig. 2A and B). The Ca salts' effect on the composite's modulus and UTS is directly correlated with their solubility while the effect on the composite's ductility is inversely correlated. These results agree with traditional polymer filler theory considering polymer chain crosslinking by solvated Ca^{2+} ions. Notably, sacrificial templates produced from PVOH-$Ca(C_2H_3O_2)_2$ or $CaCO_3$ com-

Please cite this article as: J. D. McNulty, C. Marti-Figueroa, F. Seipel et al., Micro-injection molded, poly(vinyl alcohol)-calcium salt templates for precise customization of 3D hydrogel internal architecture, Acta Biomaterialia, https://doi.org/10.1016/j.actbio.2019.04.050

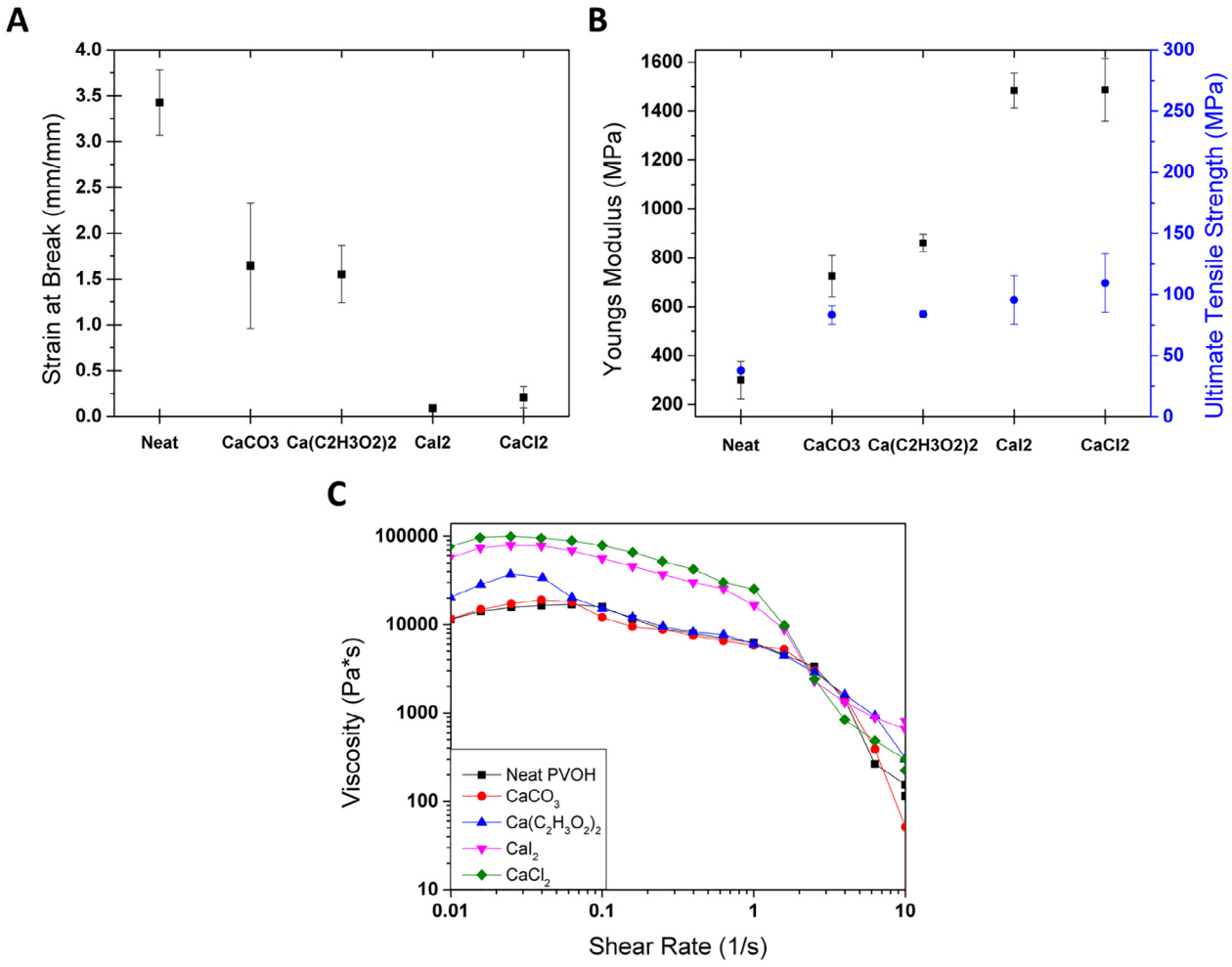

Fig. 2. PVOH-Ca composite materials' mechanical property analyzed at 25 °C. Tensile test of injection molded PVOH and PVOH-Ca materials' (A) ductility, (B) Young's modulus and ultimate tensile strength (UTS), n = 10 experimental replicates and error bars represent standard deviation. (C) Rheological analysis of each materials' viscosity over a range of shear rates.

posites versus carbohydrate glass have enhanced handling durability due to a 50-fold increase in ductility [3].

Rheological measurements were conducted to assess each PVOH-Ca composite's viscosity and thereby relative ease of manufacturing by extrusion and injection molding. Using a parallel plate rheometer to measure viscosity at continuous shear rates, PVOH-CaI_2 or -$CaCl_2$ composites displayed a viscosity ~10 fold higher than PVOH-neat, –$Ca(C_2H_3O_2)_2$, or -$CaCO_3$ across an order of magnitude shear rate range (0.1–1 per sec) (Fig. 2C). Similar to modulus and UTS data, the composite's viscosity was directly correlated to Ca salt solubility. The decreased viscosity of PVOH-neat, –$Ca(C_2H_3O_2)_2$, or –$CaCO_3$ composites was observed to facilitate extrusion and injection molding processes as well as minimized noticeable polymer degradation compared to PVOH-CaI_2 or –$CaCl_2$. As discussed later, optimizing the PVOH-Ca composite's viscosity was critical for feasible injection molding of sacrificial templates with microscale dimensions, i.e. micro-injection molding.

3.3. Optimizing calcium release properties of PVOH-Ca templates

The lower solubility of calcium acetate and carbonate salts made them ideal compounding agents for producing PVOH-Ca composites with optimal mechanical properties. However, it remained unknown how their decreased solubility would affect Ca^{2+} ion release upon composite aqueous dissolution. To calculate this quantity, we first needed to know the actual weight percent of calcium salt in each PVOH composite. Since PVOH but not the compounded calcium salts decomposes below 600 °C, thermogravimetric analysis (TGA), which measures mass loss over increasing temperatures, was conducted on PVOH compounded with 10% (w/w) calcium salts. As shown in Fig. 3A, the compounded salts persisted in the ash content at 600 °C. When normalized to the remaining neat PVOH ash, the salt masses were found to be consistent with compounded values except for the PVOH-CaI_2 composite. Considerable PVOH degradation was observed during PVOH-CaI_2 extrusion, and this likely skewed the TGA results since degraded PVOH does not burn off at 600 °C. Furthermore, the TGA curves revealed that the onset of degradation (first curve inflection point) of all PVOH-Ca composites occurred at lower temperatures than the neat composite, potentially indicating disruption of PVOH crystallinity by Ca^{2+} ions. This further corroborates the presence of intra-composite PVOH polymer/Ca^{2+} crosslinking.

A complexometric calcium titration was performed on the PVOH-Ca composites to assess the amount of Ca^{2+} ions released upon dissolution in deionized water (Fig. 3B). Calculating from the titration and TGA data, the average percent of released Ca^{2+} content was determined to never be greater than ~50%. Also, the Ca^{2+} released from PVOH-$Ca(C_2H_3O_2)_2$ or -$CaCl_2$ composites was equivalent and significantly higher than that released from PVOH-CaI_2 and -$CaCO_3$. The lower Ca^{2+} content release from PVOH-CaI_2 composites could be due to the considerable observed polymer degradation during extrusion and the skewed TGA data

Please cite this article as: J. D. McNulty, C. Marti-Figueroa, F. Seipel et al., Micro-injection molded, poly(vinyl alcohol)-calcium salt templates for precise customization of 3D hydrogel internal architecture, Acta Biomaterialia, https://doi.org/10.1016/j.actbio.2019.04.050

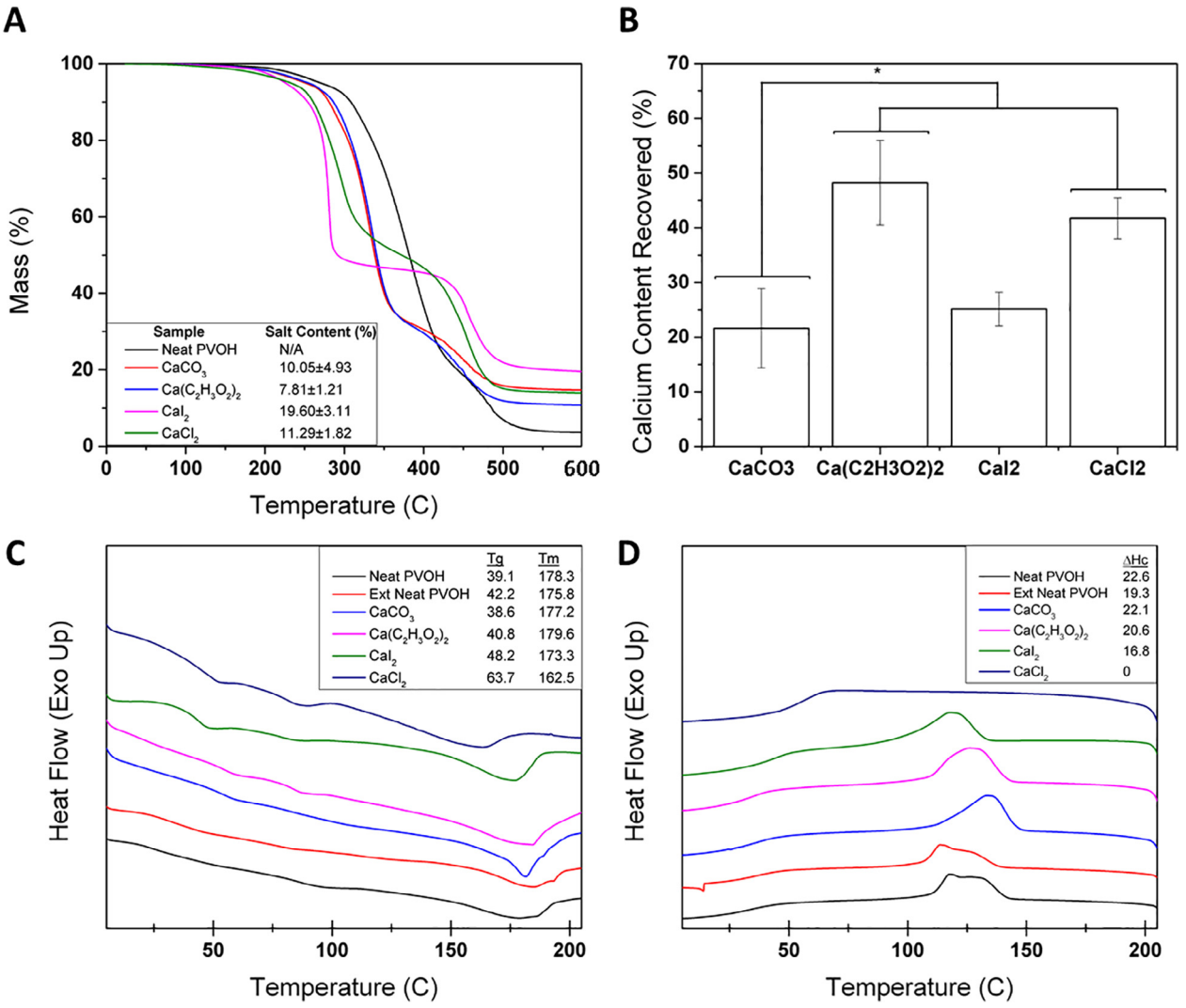

Fig. 3. Analysis of the PVOH-Ca composite composition, material, and calcium release properties. (A) Representative thermogravimetric scans, n = 3 experimental replicates. (B) Complexometric calcium titration results, n = 5 experimental replicates, $^{*}P < 0.05$, One-way ANOVA with post-hoc Tukey-Kramer test. Differential scanning calorimeter's (C) second heating and (D) first cooling curve traces of neat and extruded (Ext) PVOH and PVOH-Ca composites.

whereas that of the PVOH-$CaCO_3$ is likely due to the salt's low solubility in water (Supplemental Table S2).

As a final analysis to explain <50% calcium recovery from PVOH–$Ca(C_2H_3O_2)_2$ or –$CaCl_2$ composites, we performed differential scanning calorimetry (DSC). This analytical technique measures the thermal energy input required to induce a 1 °C temperature change in the sample, thereby allowing characterization of the composite's glass transition (T_g) and melting (T_m) temperatures and crystallization enthalpy (ΔH_c). In DSC second heating curves (Fig. 3C), the T_g is indicated by the curve's first inflection point, and the T_m is indicated by the curve's last inflection point. We observed a direct correlation between the composites' T_g and an inverse correlation between the composites' T_m relative to its calcium salt's solubility (Supplemental Table S2). Thus, crosslinking interactions between calcium ions solvated during the extrusion and injection molding process with the composite's PVOH polymers correlates directly with the salts' solubility. In the DSC cooling curve (Fig. 3D), the ΔH_c is calculated as the area under the curves' exothermic peak. In analyzing this material property, we observed an inverse correlation between the composites' ΔH_c and the compounded calcium salt's solubility. Moreover, the presence of a double exothermic peak in the neat PVOH and extruded neat PVOH samples versus the single peak in the extruded PVOH-Ca samples indicates that less types of crystals are being formed in salt containing samples. Collectively, the DSC results strongly suggest that the total compounded calcium content is not released from the PVOH-Ca composites upon dissolution due to intra-composite PVOH polymer/Ca^{2+} crosslinking which disrupts polymer crystallization. Importantly, our detailed analysis of each composites mechanical and calcium release properties imply that PVOH-$Ca(C_2H_3O_2)_2$ templates would provide enhanced sacrificial molding capabilities, handling durability, and micro-injection molding feasibility due to its comparatively high calcium ion release upon aqueous dissolution (Fig. 3B), moderate ductility (Fig. 2A–B), and low viscosity (Fig. 2C).

3.4. Micro-injection molded PVOH-$Ca(C_2H_3O_2)_2$ templates

To fabricate sacrificial templates with microscale feature dimensions, a micro-injection mold was CNC-milled in aluminum with a fiber template geometry 2.2 cm in length that immediately tapered from a 3 mm inlet/outlet diameter to a main fiber diameter of 500 μm (Fig. 4A and Supplemental Fig. S2). PVOH-$Ca(C_2H_3O_2)_2$ templates of 10% (w/w) salt loading were successfully microinjection molded. However, fabrication of equivalent PVOH-$CaCl_2$ templates failed indicating the enhanced processability of the

Please cite this article as: J. D. McNulty, C. Marti-Figueroa, F. Seipel et al., Micro-injection molded, poly(vinyl alcohol)-calcium salt templates for precise customization of 3D hydrogel internal architecture, Acta Biomaterialia, https://doi.org/10.1016/j.actbio.2019.04.050

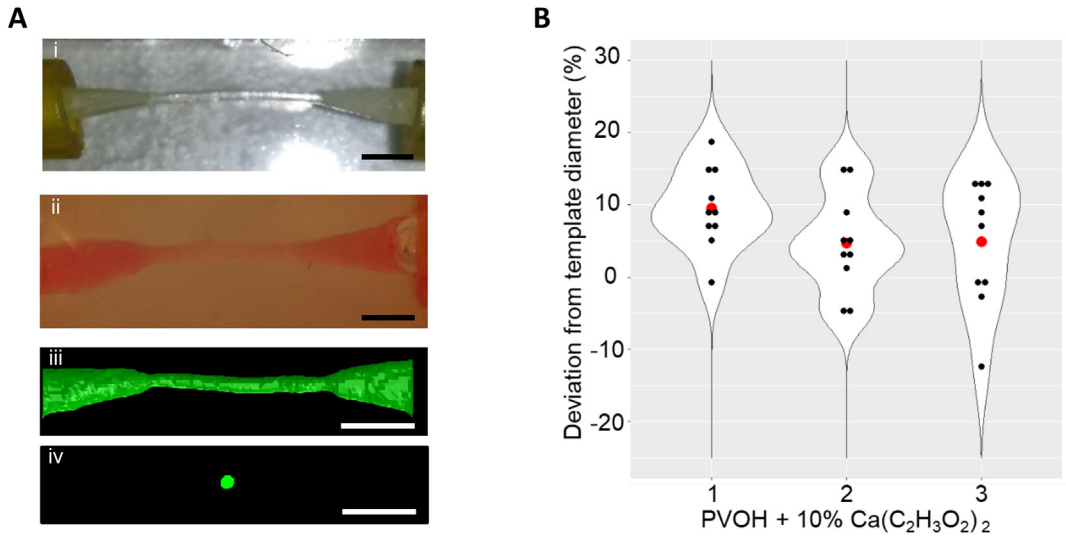

Fig. 4. Sacrificial molding using PVOH-Ca$(C_2H_3O_2)_2$ templates. Representative images of (A) micro-injection molded 10% (w/w) PVOH-Ca$(C_2H_3O_2)_2$ sacrificial fiber templates (i), the molded channel within an alginate hydrogel (ii), and a profile (iii) and cross-sectional (iv) view of the microCT-imaged channel geometry. (B) Dimensional analysis was performed on microCT scan reconstructions (A, iii and iv) of three separately cast alginate hydrogels at 10 points along each micro-channel. Black dots represent individual measurements, red dot represents the mean. Scale bars are 3 mm. (For interpretation of the references to color in this figure legend, the reader is referred to the web version of this article.)

PVOH-Ca$(C_2H_3O_2)_2$ composite material. Post sacrificial molding of alginate hydrogels using the PVOH-Ca$(C_2H_3O_2)_2$ templates, the resulting micro-channels were filled with pigmented oil for photographing, and they were quantitatively analyzed by micro-CT imaging and reconstruction analysis (Fig. 4A). Dimensional analysis of the microCT reconstructions revealed that the molded channel diameter deviated from the template geometry by an average of 6.4 ± 7.2% at any point along its long axis, i.e. 10 measurements per molded channel (Fig. 4B). This demonstrates repeatable and precise casting of microscale architecture within diffusion limited, ionically crosslinked alginate hydrogels. Additionally, similarly dimensioned neat PVOH templates left no discernable microchannel within alginate monoliths (data not shown).

3.5. Biocompatibility of the PVOH-Ca template sacrificial molding process

To verify biocompatibility of the PVOH-Ca$(C_2H_3O_2)_2$ template, H9 hESC-derived neurospheres were co-encapsulated within alginate hydrogels during the sacrificial molding process (Supplemental Fig. S3B). Neuroepithelial cells (NECs) were derived using the E6 protocol [23] and re-seeded at 180,000 cells/well in 96 well plates. The cells aggregated over 2 days of culture in E6 media to form spheroids that were collected and mixed into 2% (w/v) alginate pre-hydrogel solutions. Then, the alginate/neurosphere solution was pipetted into stainless steel hydrogel molding devices and encapsulated the suspended sacrificial PVOH-Ca$(C_2H_3O_2)_2$ template. After template dissolution over 24 hrs in E6 media under standard culture conditions, the hydrogels were fixed and sectioned to analyze cell viability within the neurospheres using TUNEL staining (Supplemental Fig. S3A). As a cell death control, a cohort of hydrogel samples were subjected to a freeze-thaw cycle prior to fixation. As a positive control, alginate hydrogels containing neurospheres in the absence of sacrificial templates were also analyzed. TUNEL staining revealed that the presence of the sacrificial template had no significant deleterious effect on cell viability compared to Freeze-Thaw (negative) and non-template (positive) controls (Supplemental Fig. S3A and C). Moreover, minimal cell death was observed during the sacrificial molding process overall (Supplemental Fig. S3A). These results indicate that the PVOH-Ca$(C_2H_3O_2)_2$ template and sacrificial molding process is compatible with standard cell culture.

3.6. Using sacrificially molded alginate hydrogels to control microscale neuroepithelial organoid morphology

Human pluripotent stem cell derived organoids have revolutionized the ability to model developmental morphogenesis in vitro. However, standard organoid derivation protocols initiate using a microscale spheroidal cell aggregate morphology, which is achieved upon spontaneous aggregation of cell suspensions but is not mimetic of many tissue-specific developmental processes [26,27]. To demonstrate an organoid engineering application of alginate hydrogels sacrificially molded using PVOH–Ca$(C_2H_3O_2)_2$ micro-fiber templates, we investigated the use of this platform to engineer neuroepithelial organoids of microscale cylindrical morphology, which is mimetic to the embryonic neural tube that gives rise to all central nervous system tissues [7].

For successful contiguous aggregate formation within such sacrificially molded alginate hydrogels, it was hypothesized that high concentration cell slurry injections into the hydrogel's molded, microscale channel is required. Thus, we investigated which H9 hESC cell slurry concentrations could be injected through a gel-loading micropipette tip without decreasing cell viability due to shear stress (Supplemental Fig. S4A). Cell suspensions of 100,000, 250,000, and 500,000 cells/μL concentrations were prepared, collected and injected by syringe pump through a gel-loading micropipette tip, and re-seeded back into Matrigel-coated 6-well plates at a 150,000 cells/cm^2 density. Observation of the cell density 24 hrs post-seeding indicated that cell slurries up to 250,000 cells/μL preserved cell viability and survival at levels comparable to the positive control which used a standard cell subculturing protocol (Supplemental Fig. S4B). Based on this result, the 250,000 cells/μL cell slurry concentration was used for injections in subsequent neuroepithelial organoid formation experiments.

In order to mimic the germinal neuroepithelial tube's tubular morphology [28], PVOH-Ca$(C_2H_3O_2)_2$, fiber templates with an elliptical cross-section of ~300 × 600 μm minor and major axes were used to sacrificially mold alginate hydrogels. H9 hESCs were injected into the alginate hydrogels' sacrificially molded channel, cultured for 24hrs in static well plate culture, and transferred to

Please cite this article as: J. D. McNulty, C. Marti-Figueroa, F. Seipel et al., Micro-injection molded, poly(vinyl alcohol)-calcium salt templates for precise customization of 3D hydrogel internal architecture, Acta Biomaterialia, https://doi.org/10.1016/j.actbio.2019.04.050

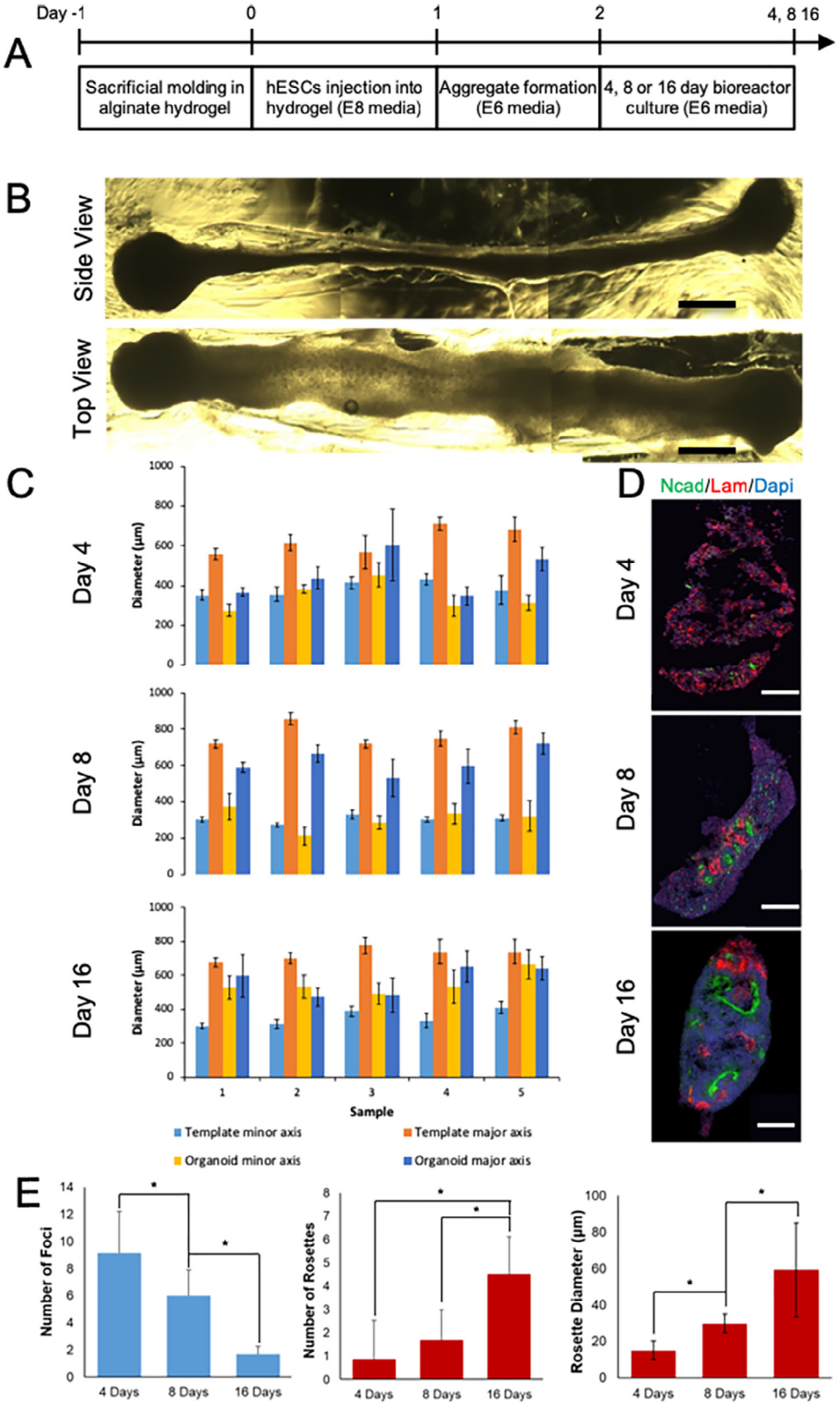

Fig. 5. Engineering neuroepithelial organoids using sacrificially molded alginate hydrogels. (A) Experimental timeline of neuroepithelial organoid derivation. Alginate hydrogels were prepared the day before injection. (B) Brightfield image of organoids after 16 days of culture demonstrating their elliptical morphology. (C) Quantification of organoid dimensions after 4, 8, and 16 days of bioreactor culture (n = 5 organoids). The PVOH-$Ca(C_2H_3O_2)_2$ template dimensions were measured before sacrificial hydrogel molding. (D) Immunocytochemistry of neuroepithelial organoid cryosections for basement membrane protein Laminin (Lam) and NEC polarization marker N-cadherin (Ncad) after 4, 8, and 16 days of bioreactor culture. (E) Quantification of the average number N-cadherin$^+$ polarization foci (left) and rosettes per cryosection (middle) and the average rosette diameter (right). Data was acquired from two organoids per day, and ~ 8 (Day 4), ~13 (Day 8), and ~ 4 (Day 16) cryosections per organoid. Error bars represent standard deviation; $^*P < 0.05$, One-way ANOVA with post-hoc Tukey-Kramer test. Scale bars are (B) 500 and (D) 100 μm.

Please cite this article as: J. D. McNulty, C. Marti-Figueroa, F. Seipel et al., Micro-injection molded, poly(vinyl alcohol)-calcium salt templates for precise customization of 3D hydrogel internal architecture, Acta Biomaterialia, https://doi.org/10.1016/j.actbio.2019.04.050

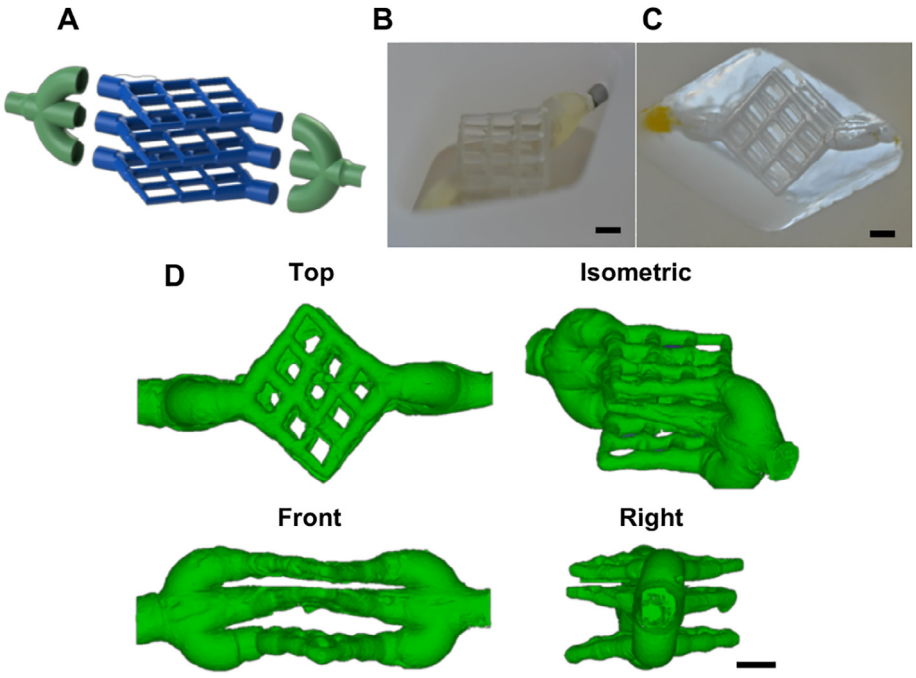

Fig. 6. Modular 3D sacrificial molding using PVOH-Ca$(C_2H_3O_2)_2$ templates. (A) Exploded CAD model of modular, 3D sacrificial template design. (B) An assembled 3D template as micro-injection molded, and (C) a sacrificially molded channel network within an alginate hydrogel. (D) microCT scanned reconstruction of the channel network within an alginate monolith. Scale bars are 3 mm.

stirred tank bioreactor culture for up to 15 additional days (Fig. 5A and B). Cylindrical cell aggregate morphology and morphogenesis were analyzed at 4, 8, and 16 days of culture. In comparison to the initial PVOH-Ca$(C_2H_3O_2)_2$ templates, the morphing aggregates' dimensions never exceed that of the template, and in many cases, appeared to contract to dimensions smaller than the molded channels over the culture period (Fig. 5B and C). Formation of polarized rings by Pax6$^+$ NECs, a.k.a. neural rosettes [23], with apical N-Cadherin$^+$ polarization and basal laminin deposition were observed by both Day 8 and 16 of bioreactor culture but largely absent at Day 4 (Fig. 5D and Supplemental Fig. S5). At Day 4 primarily small foci of N-Cadherin$^+$ polarization we observed, and as the bioreactor culture proceeded through Day 16, the number of N-Cadherin$^+$ polarization foci decreased significantly while both the number and size neural rosettes increased significantly (Fig. 5E). These results demonstrate that PVOH-Ca$(C_2H_3O_2)_2$ template-molded alginate hydrogels can be used to engineer neuroepithelial organoids, the initial phase of neural organoid derivation [29], with a biomimetic, microscale cylindrical versus spheroidal morphology. Moreover, the organoids continue to develop while cultured within alginate hydrogel molds.

3.7. Scalable 3-D molding of hydrogel architecture

Lastly, we attempted to demonstrate the injection molded PVOH-Ca$(C_2H_3O_2)_2$ templates' 3D scalability and versatility. Sacrificial templates with a manifold design that connected via an interference fit with the previous lattice geometry were fabricated (Fig. 6A). This enabled assembly of 3D PVOH-Ca$(C_2H_3O_2)_2$ templates in a Legos®-like manner (Fig. 6B), and the assembly was used to sacrificially mold 3D channel networks within polyacrylamide (Supplemental Fig. S6) and alginate hydrogels (Fig. 6C). After template dissolution, the hydrogels were scanned using a micro-CT and image reconstruction verified the resulting 3D channel networks' patency and continuity (Fig. 6D). Thus, the design and injection molding of modular, PVOH-Ca$(C_2H_3O_2)_2$ components that can be assembled into 3D sacrificial templates represents a scalable and potentially limitless approach to precisely customize the internal architecture of both bulk curing and ionically crosslinked hydrogels.

4. Discussion

The ability to engineer tissue constructs with biomimetic morphologies and cytoarchitectures has been greatly enhanced by the development of techniques to fabricate biomaterial scaffolds with macro-to-microscale features. Sacrificial molding is a promising and scalable technique for rapidly casting complex, internal architectures within hydrogel scaffolds. Yet, while previous studies demonstrated its efficacy using bulk curing hydrogels, noticeably less molding fidelity was observed when applied to diffusion limited, ionically crosslinked hydrogels such as alginate. Furthermore, these studies performed limited to no quantitative analysis of their sacrificial molding approach's feature casting fidelity [3,10,12].

Here, we fabricated injection molded, PVOH-Ca templates to facilitate and enhance sacrificial molding within ionically crosslinked hydrogels. Injection molded PVOH templates effectively mold bulk curing hydrogels such as polyacrylamide and PEG. However, the addition of calcium salts to the sacrificial templates was both necessary and sufficient to enable precise molding of microscale features within alginate monoliths. Extensive characterization unveiled that the PVOH-Ca composite mechanical, material, and calcium release properties could be tuned based on the compounded calcium salt's solubility. Also, this analysis proved that PVOH-Ca$(C_2H_3O_2)_2$ composite possessed enhanced manufacturability and sacrificial template properties, which were further demonstrated by precise casting of microscale 2D and 3D internal architecture within alginate hydrogels.

The micro-injection molded, PVOH-Ca$(C_2H_3O_2)_2$ sacrificial template's utility for tissue engineering applications was validated by its biocompatibility with cell culture and novel use to engineer neuroepithelial organoid morphology. Unlike prior efforts to engineering neural organoid morphology [30], this approach

Please cite this article as: J. D. McNulty, C. Marti-Figueroa, F. Seipel et al., Micro-injection molded, poly(vinyl alcohol)-calcium salt templates for precise customization of 3D hydrogel internal architecture, Acta Biomaterialia, https://doi.org/10.1016/j.actbio.2019.04.050

maintained a microscale cylindrical neuroepithelial organoid morphology that is mimetic of the developing neural tube [28]. While a biomimetic, singularly polarized, neuroepithelial cytoarchitecture throughout the organoid was not achieved, a recent study of micropatterned neuroepithelial tissues suggests that further optimization of the 3D neuroepithelial organoid's morphology could lead to this seminal advancement [31].

5. Conclusions

The micro-injection molded, PVOH-Ca$(C_2H_3O_2)_2$ templates described herein were developed to maximize production scalability and hydrogel engineering design versatility. We have demonstrated their applicability to sacrificial molding of both bulk-curing and ionically crosslinked hydrogel monoliths, and the templates can be mass-produced using micro-injection molding. The complexity of internal hydrogel architecture that can be molded is only limited by the need to create injection molds for each template design, which can be costly if template designs features of <300 μm are desired. Here, we demonstrated molding of channels within hydrogel monoliths but this platform can be used for any geometry, and once the PVOH-Ca$(C_2H_3O_2)_2$ templates are fabricated, the scalability of hydrogel engineering by sacrificial molding is unmatched. Modular template geometries can even be fabricated and assembled in Lego®-like configurations for rapid and precise customization of hydrogels with complex, 3D internal architecture. Finally, while we have demonstrated the platform's used for hESC-dervied neural organoid engineering, we predict that it will be highly useful for diverse tissue engineering and advanced biomanufacturing applications.

Acknowledgements

This work was supported by funding from the Wisconsin Institute for Discovery, the Wisconsin Alumni Research Foundation, the Education Foundation of the Milwaukee Section of the Society of Plastics Engineers (L.S.T), and a NSF CAREER Award #1651645 (R.S.A).

Appendix A. Supplementary data

Supplementary data to this article can be found online at https://doi.org/10.1016/j.actbio.2019.04.050.

References

[1] T.J. Hinton, Q. Jallerat, R.N. Palchesko, J.H. Park, M.S. Grodzicki, H.-J. Shue, M.H. Ramadan, A.R. Hudson, A.W. Feinberg, Three-dimensional printing of complex biological structures by freeform reversible embedding of suspended hydrogels, Sci. Adv. 1 (2015) e1500758.
[2] P. Kerscher, I.C. Turnbull, A.J. Hodge, J. Kim, D. Seliktar, C.J. Easley, K.D. Costa, E. A. Lipke, Direct hydrogel encapsulation of pluripotent stem cells enables ontomimetic differentiation and growth of engineered human heart tissues, Biomaterials 83 (2016) 383–395.
[3] J.S. Miller, K.R. Stevens, M.T. Yang, B.M. Baker, D.-H.T. Nguyen, D.M. Cohen, E. Toro, A.A. Chen, P.A. Galie, X. Yu, R. Chaturvedi, S.N. Bhatia, C.S. Chen, Rapid casting of patterned vascular networks for perfusable engineered three-dimensional tissues, Nat. Mater. 11 (2012) 768–774.
[4] J.P. Vacanti, R. Langer, Tissue engineering: the design and fabrication of living replacement devices for surgical reconstruction and transplantation, Lancet 354 (1999) S32–S34, https://doi.org/10.1016/S0140-6736(99)90247-7.
[5] R.S. Ashton, A. Banerjee, S. Punyani, D.V. Schaffer, R.S. Kane, Scaffolds based on degradable alginate hydrogels and poly(lactide-co-glycolide) microspheres for stem cell culture, Biomaterials 28 (2007) 5518–5525.
[6] J.G. Fernandez, A. Khademhosseini, Micro-masonry: construction of 3D structures by microscale self-assembly, Adv. Mater. 22 (2010) 2538–2541.
[7] S.F. Gilbert, Developmental Biology, 10 ed., Sinauer Associates Inc, Sunderland, 2014.
[8] T.S. Karande, J.L. Ong, C.M. Agrawal, Diffusion in musculoskeletal tissue engineering scaffolds: design issues related to porosity, permeability, architecture, and nutrient mixing, Ann. Biomed. Eng. 32 (2004) 1728–1743.
[9] D.B. Kolesky, R.L. Truby, A.S. Gladman, T.A. Busbee, K.A. Homan, J.A. Lewis, 3D bioprinting of vascularized, heterogeneous cell-laden tissue constructs, Adv. Mater. Weinheim. 26 (2014) 3124–3130.
[10] L.M. Bellan, S.P. Singh, P.W. Henderson, T.J. Porri, Fabrication of an artificial 3-dimensional vascular network using sacrificial sugar structures, Soft Matter 5 (2009) 1354–1357.
[11] W. Wu, C.J. Hansen, A.M. Aragón, P.H. Geubelle, S.R. White, J.A. Lewis, Direct-write assembly of biomimetic microvascular networks for efficient fluid transport, Soft Matter 6 (2010) 739–742.
[12] A. Tocchio, M. Tamplenizza, F. Martello, I. Gerges, E. Rossi, S. Argentiere, S. Rodighiero, W. Zhao, P. Milani, C. Lenardi, Versatile fabrication of vascularizable scaffolds for large tissue engineering in bioreactor, Biomaterials 45 (2015) 124–131.
[13] X.-Y. Wang, Z.-H. Jin, B.-W. Gan, S.-W. Lv, M. Xie, W.-H. Huang, Engineering interconnected 3D vascular networks in hydrogels using molded sodium alginate lattice as the sacrificial template, Lab Chip 14 (2014) 2709–2716.
[14] A.P. Golden, J. Tien, Fabrication of microfluidic hydrogels using molded gelatin as a sacrificial element, Lab Chip 7 (2007) 720–726.
[15] M.P. Cuchiara, A.C.B. Allen, T.M. Chen, J.S. Miller, J.L. West, Multilayer microfluidic PEGDA hydrogels, Biomaterials 31 (2010) 5491–5497.
[16] A. Banerjee, M. Arha, S. Choudhary, R.S. Ashton, S.R. Bhatia, D.V. Schaffer, R.S. Kane, The influence of hydrogel modulus on the proliferation and differentiation of encapsulated neural stem cells, Biomaterials 30 (2009) 4695–4699.
[17] J.A. Rowley, G. Madlambayan, D.J. Mooney, Alginate hydrogels as synthetic extracellular matrix materials, Biomaterials 20 (1999) 45–53.
[18] Z. Chen, L.-S. Turng, A review of current developments in process and quality control for injection molding, Adv. Polym. Tech. 24 (2005) 165–182.
[19] S.J. Liu, Y.S. Chen, Water-assisted injection molding of thermoplastic materials: effects of processing parameters, Polym. Eng. Sci. 43 (2003) 1806–1817.
[20] T.A. Osswald, L.-S. Turng, P.J. Gramann, Injection molding handbook, Munich, Carl Hanser Publishers: Hanser Gardner Publications, Cincinnati, 2008.
[21] A.C.D.-2.O. Plastics, D638: Standard test method for tensile properties of plastics. West Conshohocken (PA): ASTM International, 2010.
[22] M.W. Toepke, N.A. Impellitteri, J.M. Theisen, W.L. Murphy, Characterization of thiol-ene crosslinked PEG hydrogels, Macromol. Mater. Eng. 298 (2012) 699–703.
[23] E.S. Lippmann, M.C. Estevez-Silva, R.S. Ashton, Defined human pluripotent stem cell culture enables highly efficient neuroepithelium derivation without small molecule inhibitors, Stem Cells 32 (2014) 1032–1042.
[24] S.R. Peyton, C.B. Raub, V.P. Keschrumrus, A.J. Putnam, The use of poly(ethylene glycol) hydrogels to investigate the impact of ECM chemistry and mechanics on smooth muscle cells, Biomaterials 27 (2006) 4881–4893.
[25] A.A. Bonapasta, F. Buda, P. Colombet, G. Guerrini, Cross-linking of poly(vinyl alcohol) chains by Ca ions in macro-defect-free cements, Chem. Mater. 14 (2002) 1016–1022.
[26] M.A. Lancaster, J.A. Knoblich, Organogenesis in a dish: modeling development and disease using organoid technologies, Science 345 (2014). 1247125–1 1247125-9.
[27] C.R. Marti-Figueroa, R.S. Ashton, The case for applying tissue engineering methodologies to instruct human organoid morphogenesis, Acta Biomater. 54 (2017) 35–44.
[28] S.A. Bayer, J. Altman, Atlas of Human Central Nervous System Development, CRC Press, Boca Raton, 2002.
[29] M.A. Lancaster, M. Renner, C.-A. Martin, D. Wenzel, L.S. Bicknell, M.E. Hurles, T. Homfray, J.M. Penninger, A.P. Jackson, J.A. Knoblich, Cerebral organoids model human brain development and microcephaly, Nature 501 (2013) 373–379.
[30] M.A. Lancaster, N.S. Corsini, S. Wolfinger, E.H. Gustafson, A.W. Phillips, T.R. Burkard, T. Otani, F.J. Livesey, J.A. Knoblich, Guided self-organization and cortical plate formation in human brain organoids, Nat. Biotechnol. 35 (2017) 659–666.
[31] G.T. Knight, B.F. Lundin, N. Iyer, L.M. Ashton, W.A. Sethares, R.M. Willett, R.S. Ashton, Engineering induction of singular neural rosette emergence within hPSC-derived tissues, Elife 7 (2018) e37549.

Please cite this article as: J. D. McNulty, C. Marti-Figueroa, F. Seipel et al., Micro-injection molded, poly(vinyl alcohol)-calcium salt templates for precise customization of 3D hydrogel internal architecture, Acta Biomaterialia, https://doi.org/10.1016/j.actbio.2019.04.050